GSA DR2009254

Data Repository for:

Timing and structure of the 8.2 ky event inferred from $\delta^{18}O$ records of stalagmites from China, Oman and Brazil.

By Cheng et al., 2009

1. Analytical Methods

The chemical procedures used to separate the uranium and thorium for ^{230}Th dating are similar to those described in Edwards et al. (1987). ^{230}Th dating of stalagmites was made at the Minnesota Isotope Laboratory, University of Minnesota, USA. The dating procedure using the ICP-MS, Thermo-Finnigan Element, is described in Shen et al. (2002). Here we provide detail information of the dating procedure using a multi-collector inductively coupled plasma mass spectrometers (MC-ICP-MS, Thermo-Finnigan Neptune) (also see Cheng et al., 2008 and 2009). The general instrumentation information about Neptune is well described by Wieser and Schwieters (2005). The Neptune collector system consists of eight moveable Faraday cups and a fixed centre cup. The axial beam can be deflected into either the central Faraday cup or a secondary electron multiplier (SEM, a MasCom multiplier). The SEM is located behind an energy and angular filtering device (Retarding Potential Quadrupole – RPQ) to achieve better abundance sensitivity. The usage of RPQ can be chosen by applying high voltages or grounding. The Neptune was operated at low resolution ($M/\Delta M \approx 300$). Radio frequency (RF) power was set at ~1200 Watts. The skimmer cone is the X-cone from the Elemental Scientific Inc. (ESI). Argon flow rates were set at 15 l/min for plasma gas, 0.8–1.0 l/min for auxiliary gas and 0.8-1.0 l/min for sample gas. We chose a dry sample introduction system, CETAC Aridus or Aridus-II, which reduces the interferences from oxides and hydrides in comparison with wet introduction systems. The nebulizer (ESI-50) has an uptake rate of 70-50 μl/min for cup measurements and (ESI-20) 20-40 μl/min for SEM measurements, respectively. The sweep Ar flow was typically set at 5–6 l/min and nitrogen between 0.08–0.15 l/min. The temperatures of the spray chamber and desolvator were set at 110 ºC and 160 ºC, respectively. This system provided a high overall sensitivity, ionization plus transmission efficiencies, on an order of 1–2 % for both U and Th, resulting in a significant increase in dating precision.

All Faraday cup measurements of uranium isotopes were carried out by cups with tails corrected by measuring background at half mass and masses at 234.5 and 237 using a MasCom multiplier. The cup configurations are as following: one sub-configuration measuring ^{233}U–^{234}U–^{235}U–^{236}U–^{238}U on Faraday cups on a static mode and two sub-configurations measuring tails at masses 234.5 and 237.0 on the axial SEM without using the RPQ. The smallest uranium isotope (^{234}U) beam intensities are measured at ~30 mV. The mass fractionations were determined by measuring intensities of masses ^{233}U and ^{236}U from a ^{233}U–^{236}U double spike. The SEM dark noise of ~0.02 cps and the yield with daily variability of ≤ 1% were routinely monitored during daily measurements. U and Th tailing characteristics were carefully addressed and corrected in an off-line data reduction process, modified from Shen et al. (2002). The uncertainty of tailing effect of less than

2% is approximately equivalent to an error of ≤ 1 ε on ^{234}U measurement. It can be further reduced by carefully charactering the tailing effects. The ^{238}U was measured with a cup which is associated with an amplifier fitted with a positive feedback resistor of 10^{10} Ω, different from the rest standard resistors of 10^{11} Ω. The ^{238}U beam intensity can then be measured at ~50 V (on a 10^{10} Ω resistor which is equivalent to 500 V on a 10^{11} Ω resistor), or the minor U isotope (^{234}U) beam to be measured simultaneously at an intensity of ~30 mV. The baselines of the Faraday cups were also measured prior to and after each U measurement for 12 minutes, approximately the same time as U-measurement or more. The uncertainties of baselines are generally within ±3.5 μV for both internal measurements and daily external reproducibility.

We use the technique of SEM measurement for Th isotopes. The technique is, in general, similar to those described by Cheng et al. (2000) and Shen et al. (2002). Measurements of Th fractions were made on the central SEM behind the RPQ. The dead time value of the SEM is about 20 ns for the MasCom multiplier. Following the same method used in Cheng et al (2000), we determine for the SEM dead time with a precision of ~0.5 ns by measuring a set of aliquots with different U concentrations from a same U standard solution. To further reduce dead-time uncertainty, we set the largest beam intensity at ~300,000 cps for sample measurements, except ^{232}Th beam, as the ^{232}Th measurements are used to monitor detrital contamination and the analytical error is secondary in comparison to the uncertainty in detrital $^{230}Th/^{232}Th$. Jumping mode was used to measure ^{229}Th–^{230}Th–^{232}Th, unless ^{232}Th beams are very high. Mass biases were corrected by bracketing measurements of ^{236}U–^{233}U double spike (Shen et al., 2002). The intensity biases associated with the SEM are similar to what we have observed before for the same type of multiplier (Cheng et al., 2000) and were characterized using the same methods as described by Cheng et al. (2000) and Shen et al. (2002). In addition, we also routinely check a set of our four in-house Th standards, with $^{230}Th/^{229}Th$ ratios range between 0.00454 – 0.1765, and spiked NBL-112A uranium standard to monitor the consistency of daily analytical results.

All dates are in stratigraphic order within analytical errors. Typical dating errors are between 15 and 45 years at most key points around the 8.2 ky event (Table S1; Figure S2), compatible to Greenland ice core errors and a factor of 3 to 5 times better than the most previous dating of the event anomalies.

The analytical procedures of oxygen isotope ratios ($^{18}O/^{16}O$) of samples D4 and DA are similar to those described in Dykoski et al. (2005) and Wang et al. (2005) respectively. The new oxygen isotope ratios were measured in three locations: (1) the College of Geography, Nanjing Normal University, China (Q5 and PAD07) using a Finnigan-MAT 253 mass spectrometer fitted with a Kiel Carbonate Device III; (2) the Institute of Geological Sciences, University of Bern, Switzerland (H14) using a VG Prism linked to an on-line automatic carbonate system; and (3) the University of São Paulo, Brazil (PX5) using a Finnigan Delta Plus Advantage with an on-line automatic carbonate preparation system. Data were calibrated against standards NBS-18 and NBS-19 and are reported as $\delta^{18}O$ (‰) relative to the Vienna Pee Dee Belemnite (VPDB). Duplicates were analyzed every 10 to 20 samples to check for homogeneity, all of which replicated within 0.15‰.

2. Figures

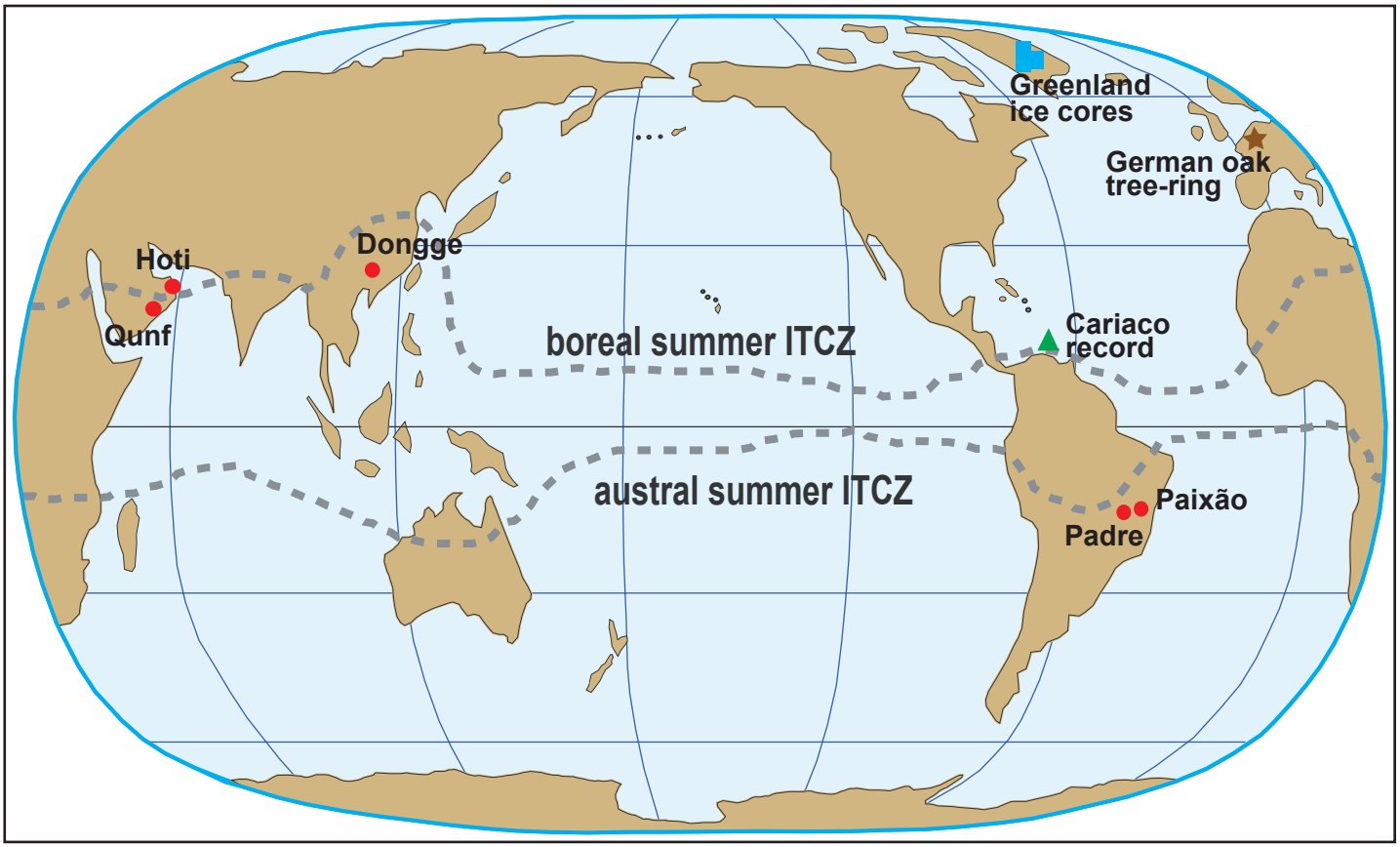

Figure DR1. Locations of five caves in this study. Red dots indicate locations of Dongge Cave, China (25º17'N, 108º5'E), Hoti Cave, Oman (23°05'N, 57°21'E), Qunf Cave, Oman (17°10'N, 54°18'E), Padre Cave, Brazil (13º13'S, 44º3'W) and Paixão Cave, Brazil (12º39'S, 41º3'W). Dongge, Qunf and Hoti caves are located in the Asian Monsoon (AM) region, and Padre and Paixão caves in the South American Summer Monsoon (SASM) region. Locations of Greenland ice cores, the Cariaco Basin sediment record and the German oak tree-ring record are also depicted with blue squares, green triangle and brown star respectively. The approximate seasonal shift of the Intertropical Convergence Zone (ITCZ) is indicated by two dashed lines.

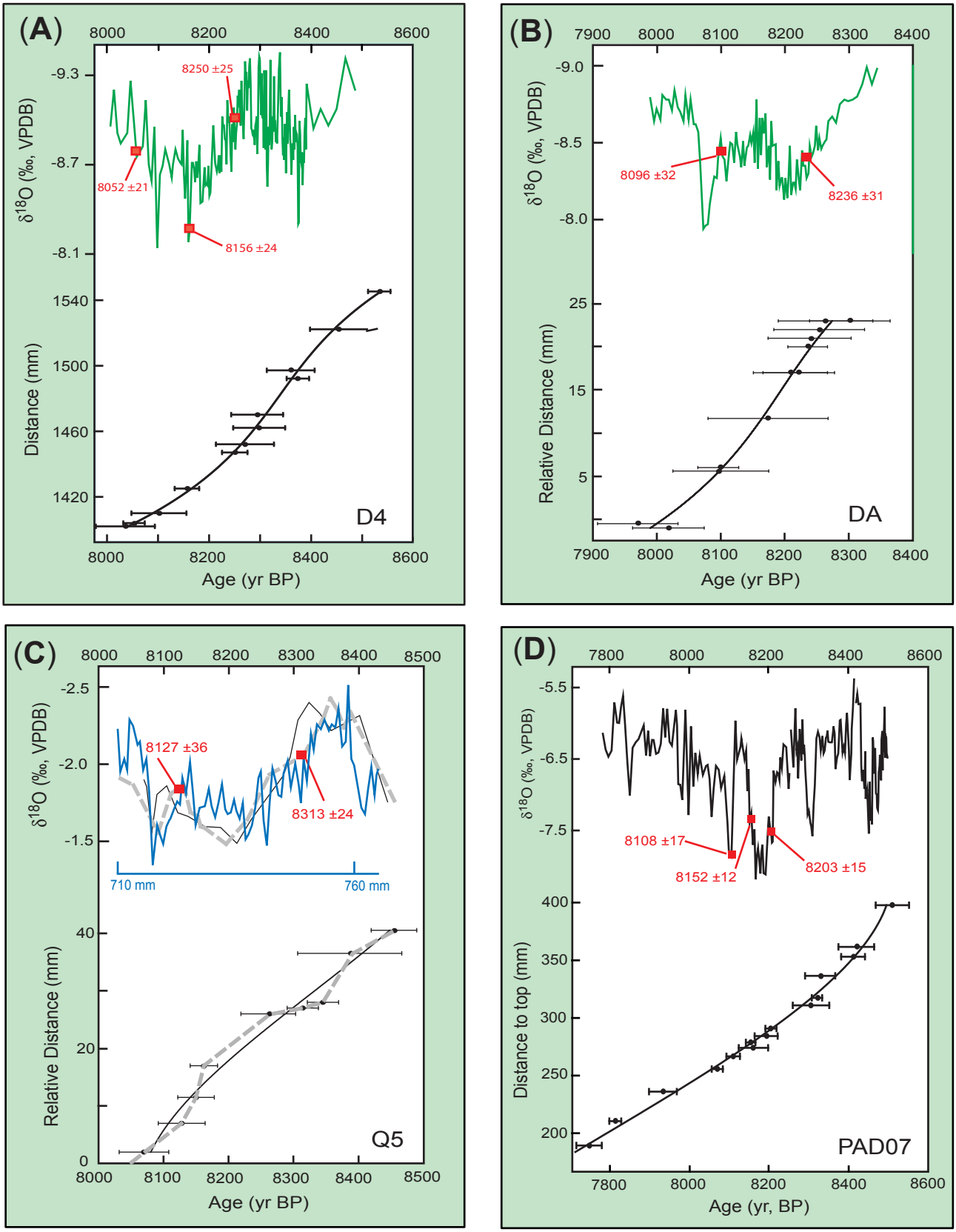
(A)
8250 ±25
8052 ±21
8156 ±24
δ18O (‰, VPDB)
Distance (mm)
D4
Age (yr BP)
(B)
8096 ±32
8236 ±31
δ18O (‰, VPDB)
Relative Distance (mm)
DA
Age (yr BP)
(C)
8127 ±36
8313 ±24
710 mm
760 mm
δ18O (‰, VPDB)
Relative Distance (mm)
Q5
Age (yr BP)
(D)
8108 ±17
8152 ±12
8203 ±15
δ18O (‰, VPDB)
Distance to top (mm)
PAD07
Age (yr, BP)

Figure DR2

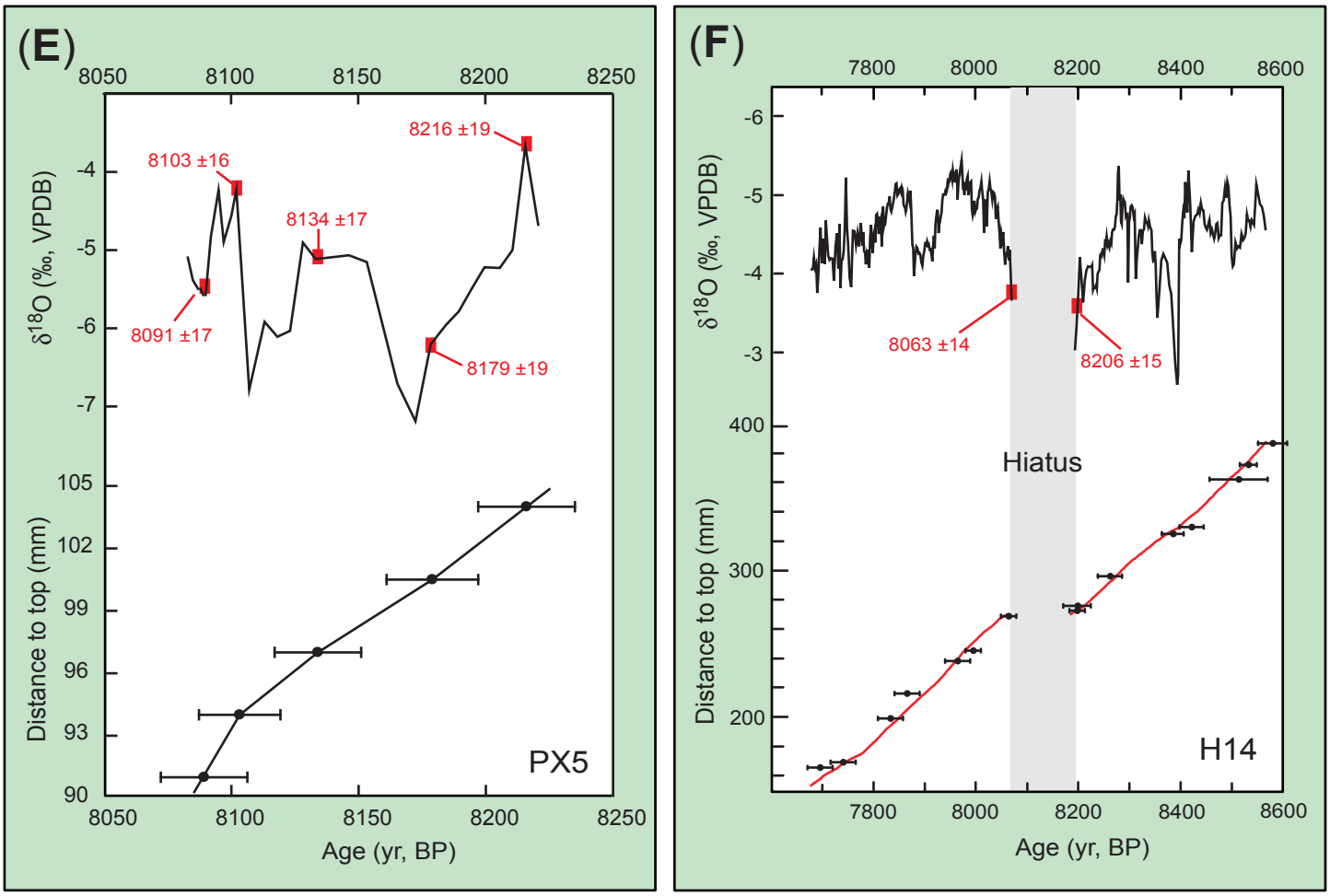

Figure DR2. Age models of stalagmites D4 (**A**) and DA (**B**) from Dongge Cave, China, Q5 from Qunf Cave, Oman (**C**), PAD07 from Padre Cave, Brazil (**D**), PX5 from Paixão Cave, Brazil (**E**) and H14 from Hoti Cave, Oman (**F**). Age models of D4, DA and PAD07 are based on polynomial (cubic) fitting of ^{230}Th dating results and essentially identical to linear interpolation methods around the 8.2 ky event. The chronology of sample Q5 is obtained by linear interpolations between two ^{230}Th dates (dashed gray curve) which is similar to the chronology using polynomial (cubic) fitting method (black line). The previous Q5 δ^{18}O record (Fleitmann et al., 2003) was plotted on distance scale (blue line) and it broadly matches the new chronology (dashed gray or black curves). The age model of PX5 is simply obtained by linear interpolations between five dates. The age model of sample H14 is established using both ^{230}Th dating (absolute age) and annual growth band counting (relative age) and ^{230}Th dating chronology agrees with band counting results within errors. The gray bar shows a hiatus in sample H14. Some critical ^{230}Th dates and errors are shown with numbers in red.

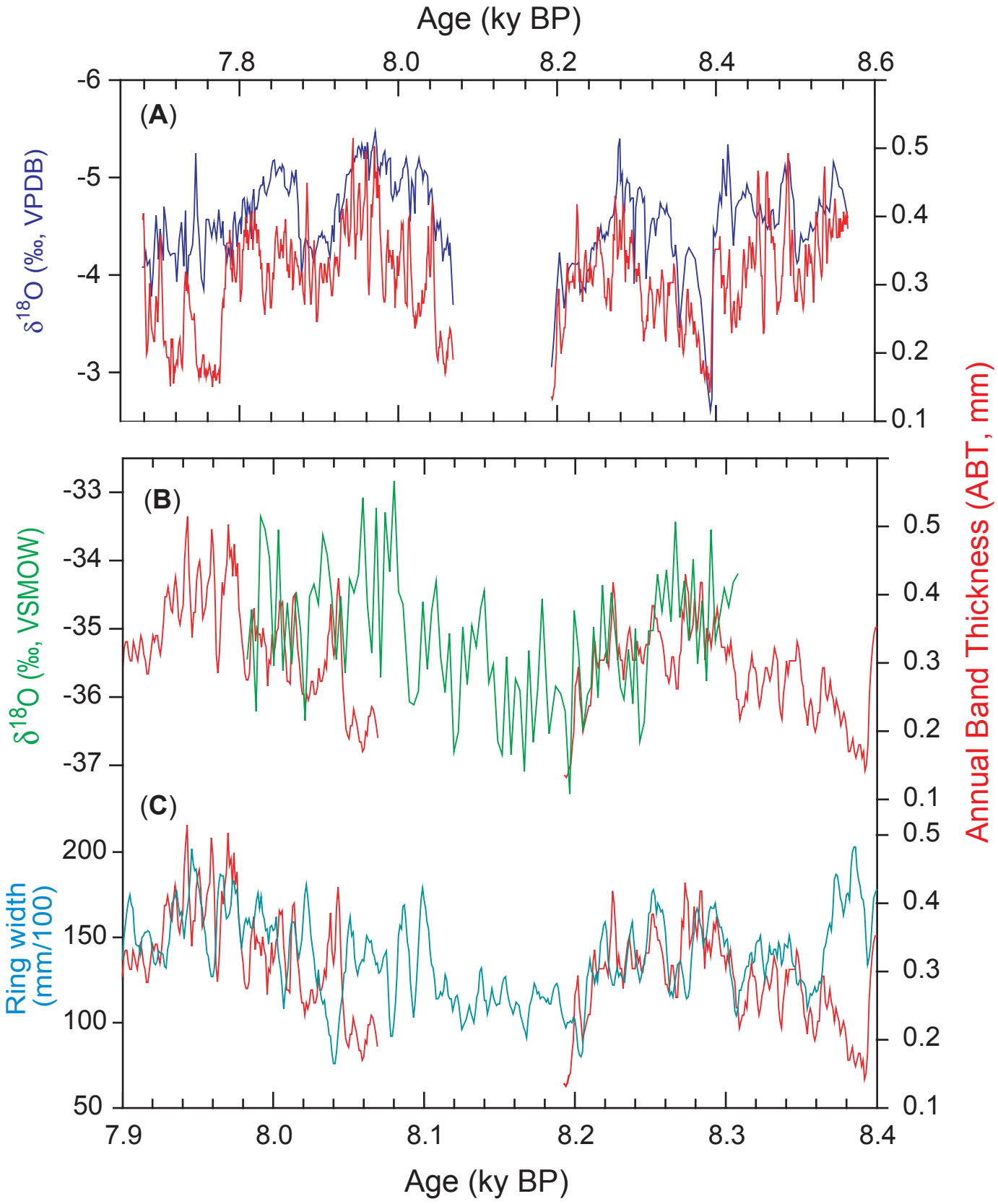

Figure DR3. (**A**) Comparison between $\delta^{18}O$ and annual band thickness (ABT) in stalagmite H14. (**B**) Comparison between stalagmite H14 ABT profile and NGRIP $\delta^{18}O$ profile (Rasmussen et al., 2006); (**C**) Comparison between stalagmite H14 ABT profile and German oak tree-ring chronology (Spurk et al., 2002).

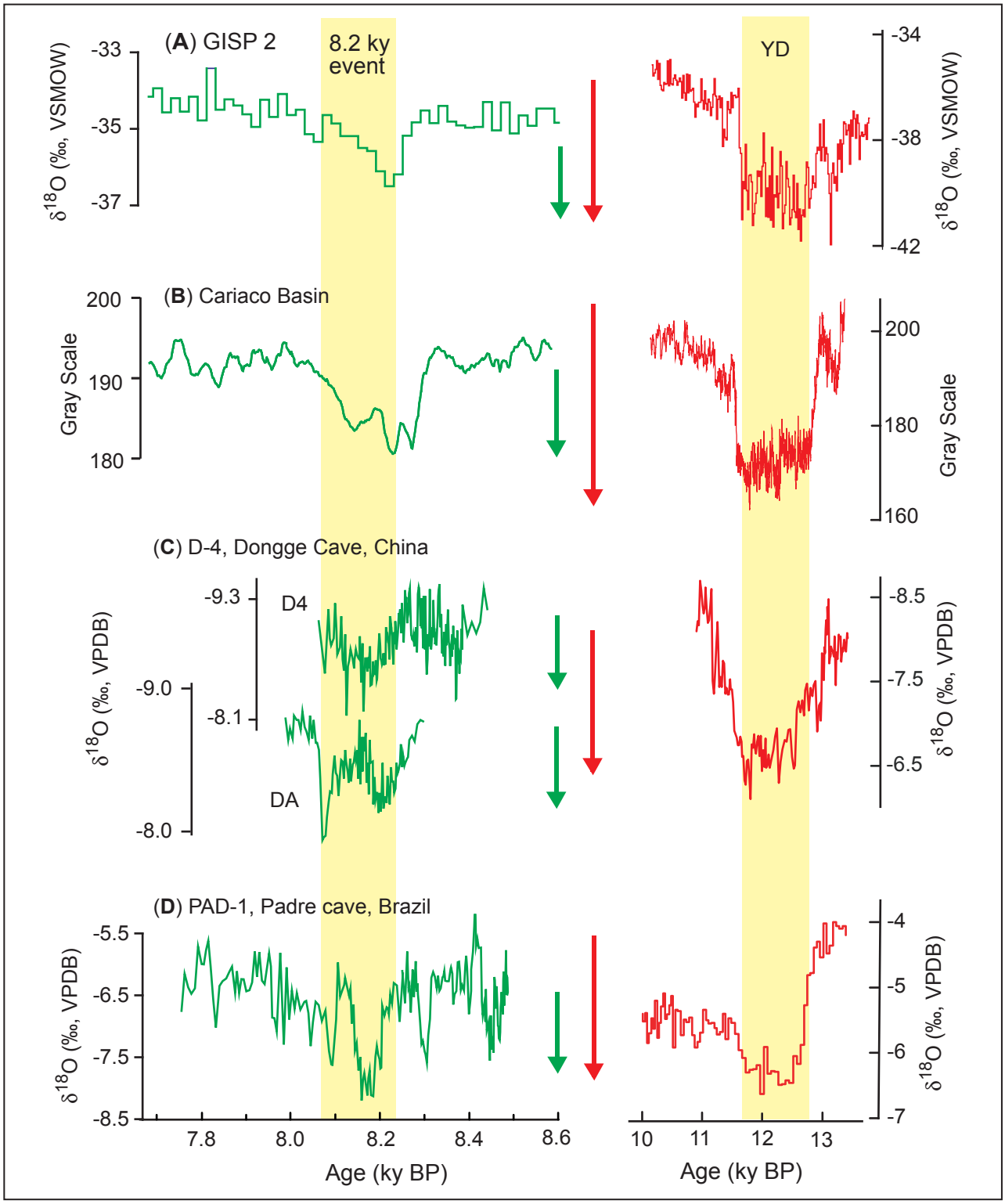

Figure DR4. Climate proxy records of the 8.2 ky and the Younger Dryas (YD) events. (**A**) $\delta^{18}O$ record of Greenland ice core (GISP2, Stuiver and Grootes 2000). (**B**) The sediment grayscale record from the Cariaco Basin, offshore Venezuela (Hughen et al., 1996). (**C**) $\delta^{18}O$ records of stalagmites D4 and DA (Dykoski et al., 2005; Wang et al., 2005). (**D**) The $\delta^{18}O$ record of stalagmites PAD07 (Wang et al., 2007). Red and green arrows indicate changes and amplitudes of the Younger Dryas (YD) and the 8.2 ky events respectively in Greenland temperature (**A**), increased zonal wind speed in the Cariaco Basin due to high-latitude cooling (**B**), weakening in the Asian Monsoon (**C**) and strengthening in the South American Summer Monsoon (**D**). Similar to scenarios recorded by Greenland ice core and Cariaco Basin records, the 8.2 kys event in both Asian Monsoon and South American Summer Monsoon records are analogous to the YD cold event with amplitudes approximately half of their YD event.

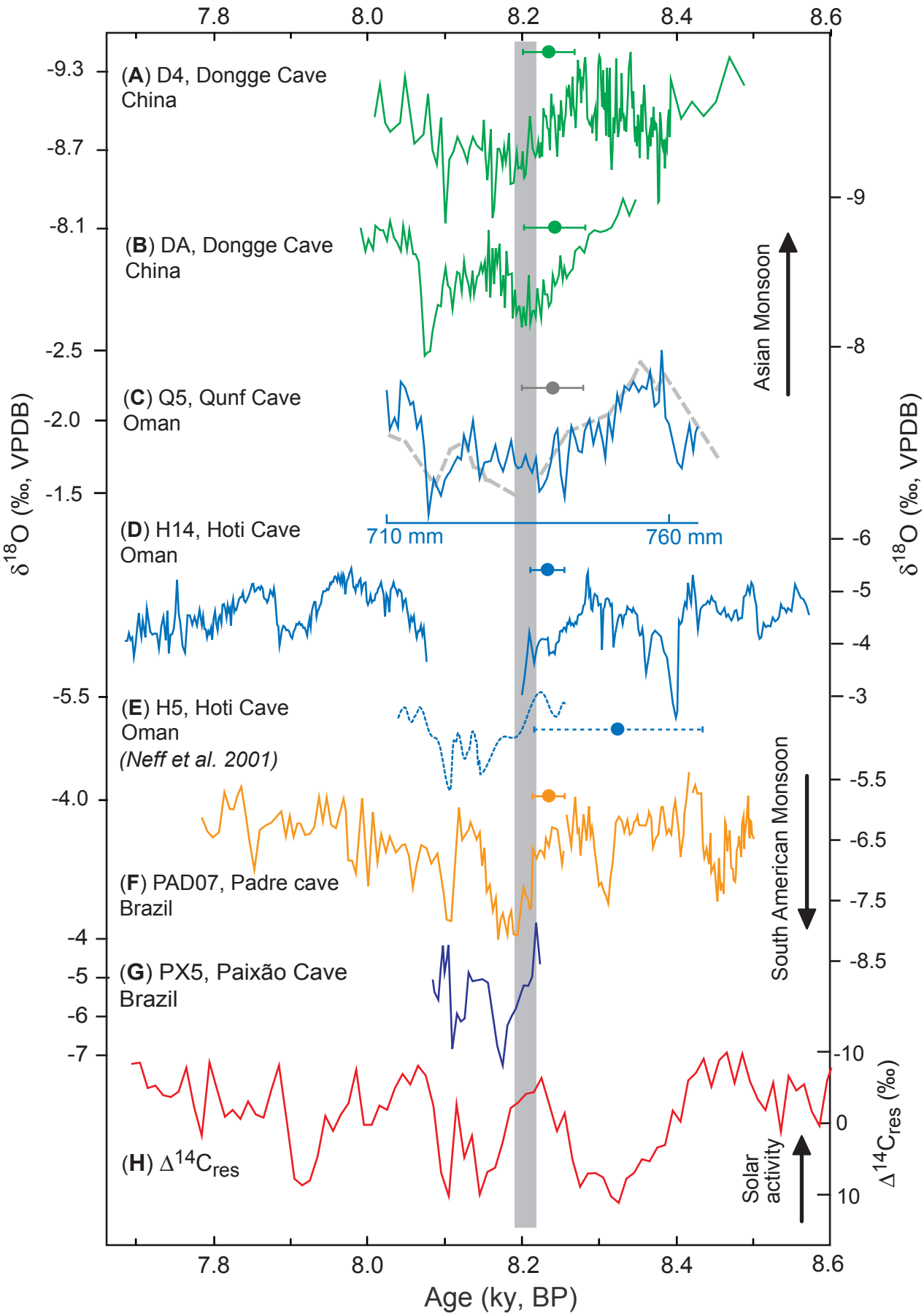

Figure DR5. Comparison among variations in the Asian Monsoon (**A**-**E**), the South American summer monsoon (**F**-**G**) and the detrended atmospheric $\Delta^{14}C_{res}$ profile (**H**) (Stuiver et al., 1998) around the 8.2 ky event. The grey vertical bar indicates the timing of the onset of the event in Asian Monsoon and the South American Summer Monsoon records. It appears that the 8.2 ky event occurred when solar activity was relatively strong.

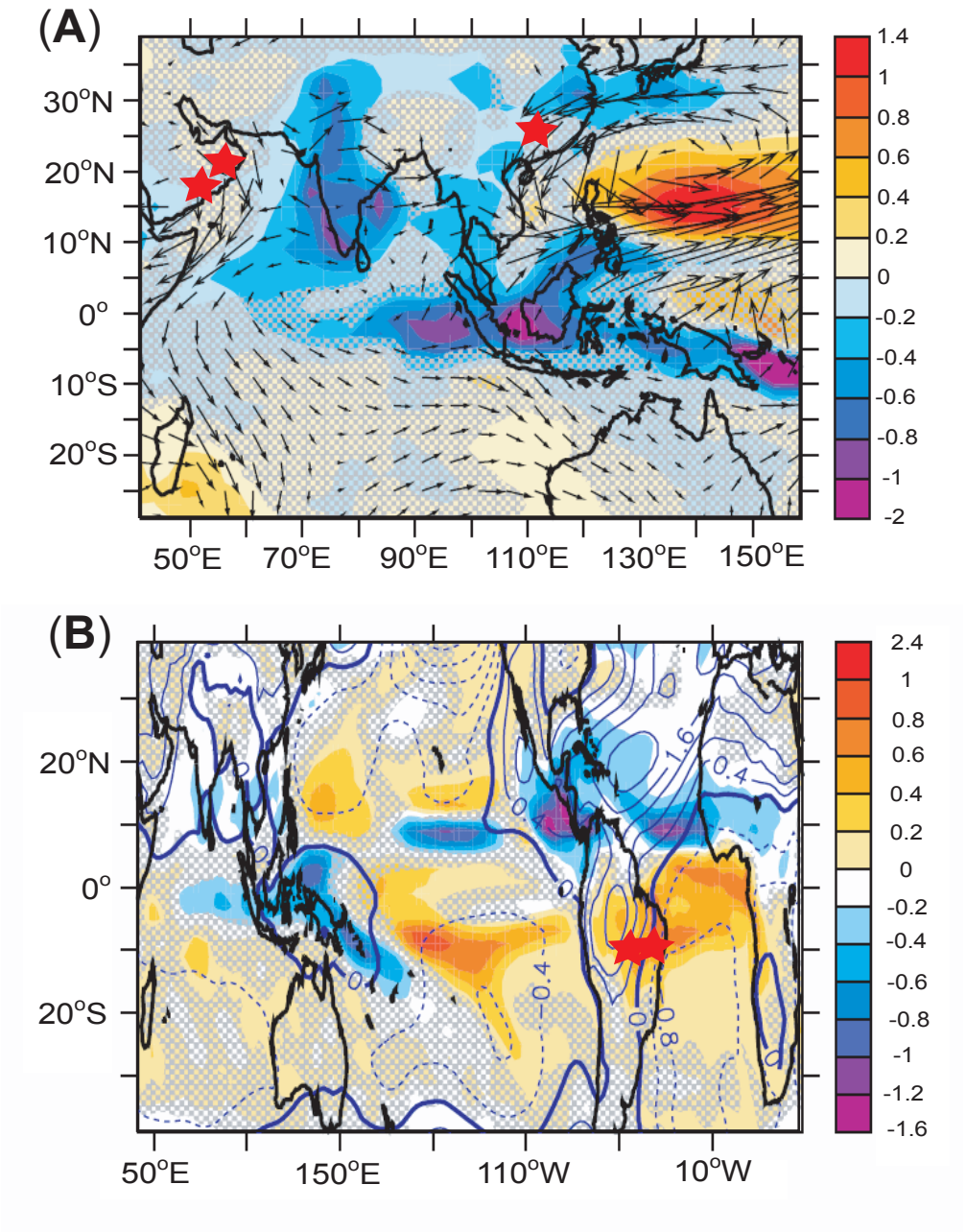

Figure DR6. Simulated tropical responses to a substantial weakening of the Atlantic Meridional Overturning Circulation (AMOC) (Zhang and Delworth 2005). (**A**) Anomalous summer precipitation (myr^{-1}) and flow at 925 hPa over the Asian Monsoon regions. Red stars mark three cave locations in the region (i.e. Dongge, Qunf and Hoti caves, see Fig. DR1). (**B**) Annual mean precipitation anomaly over South America (myr^{-1}). Two red stars mark locations of Padre and Paixão caves, eastern Brazil.

3. Tables

Table DR1. ^{230}Th dating results. All errors are reported at the 2σ level of uncertainty.

Sample Number	Depth to top (mm)	^{238}U ppb	^{232}Th ppt	^{230}Th / ^{232}Th atomic x10^{-6}	δ^{234}U* measured	^{230}Th / ^{238}U activity	Age (yr) uncorrected	Age (yr) corrected	$\delta^{234}U_{Initial}$ (corrected)	Age (yr, BP)** corrected
D4, Dongge Cave, China										
D4-4	1402	356.0 ±0.5	62 ±5	6700 ±600	-26.0 ±1.8	0.06977 ±0.00046	8101 ±58	8091 ±58	-26.6 ±1.9	**8035 ±58**
D4-9 [n]	1404	388.0 ±0.1	89 ±4	5000 ±200	-23.9 ±1.2	0.07009 ±0.00014	8120 ±19	8108 ±21	-24.5 ±1.2	**8052 ±21**
D4-1	1410	497.2 ±0.8	468 ±6	1240 ±20	-26.3 ±1.5	0.07063 ±0.00035	8206 ±44	8157 ±54	-26.9 ±1.6	**8101 ±54**
D4-8 [n]	1425	493.8 ±0.1	191 ±5	3020 ±80	-28.8 ±0.5	0.07065 ±0.00016	8232 ±20	8212 ±24	-29.5 ±0.5	**8156 ±24**
D4-10 [n]	1447	370.5 ±0.1	143 ±5	3100 ±100	-13.2 ±0.7	0.07259 ±0.00017	8326 ±21	8306 ±25	-13.5 ±0.7	**8250 ±25**
D4-5	1452	333.0 ±0.4	67 ±4	6000 ±400	-9.8 ±2.0	0.07293 ±0.00045	8336 ±56	8326 ±57	-10.1 ±2.0	**8270 ±57**
D4-2	1462	463.5 ±0.7	329 ±6	1700 ±30	-10.7 ±1.5	0.07333 ±0.00036	8391 ±45	8354 ±51	-10.9 ±1.5	**8298 ±51**
D4-6	1470	305.1 ±0.3	170 ±3	2150 ±40	-18.9 ±1.7	0.07262 ±0.00038	8379 ±48	8350 ±51	-19.3 ±1.7	**8294 ±51**
D4-11 [n]	1492	359.8 ±0.1	96 ±4	4600 ±200	-10.1 ±0.7	0.07382 ±0.00016	8444 ±20	8430 ±22	-10.3 ±0.7	**8374 ±22**
D4-3	1497	434.6 ±0.6	232 ±6	2280 ±60	-8.9 ±1.4	0.07389 ±0.00035	8443 ±43	8416 ±47	-9.2 ±1.4	**8360 ±47**
D4-7	1522	359.8 ±0.4	199 ±6	2220 ±70	-12.3 ±1.6	0.07444 ±0.00043	8539 ±53	8510 ±56	-12.6 ±1.7	**8454 ±56**
D4-12 [n]	1545	384.8 ±0.1	140 ±3	3400 ±80	-10.4 ±0.6	0.07518 ±0.00015	8609 ±19	8590 ±22	-10.7 ±0.6	**8534 ±22**
DA, Dongge Cave, China										
DA5-13	858.5	586.3 ±0.8	570 ±5	1140 ±10	-69.9 ±1.7	0.06679 ±0.00033	8126 ±44	8073 ±56	-71.5 ±1.7	**8018 ±56**
DA5-6	859.0	545.6 ±0.7	200 ±10	2900 ±200	-72.9 ±1.1	0.06594 ±0.00048	8046 ±61	8025 ±63	-74.5 ±1.2	**7970 ±63**
DA5-5	865.1	615.3 ±0.8	590 ±10	1150 ±30	-75.3 ±1.2	0.06705 ±0.00051	8209 ±66	8156 ±75	-77.1 ±1.2	**8101 ±75**
DA-17 [n]	865.5	752.3 ±0.1	689 ±5	1210 ±10	-74.8 ±0.7	0.06703 ±0.00015	8201 ±20	8151 ±32	-76.5 ±0.7	**8096 ±32**
DA5-4	871.2	516.2 ±0.8	340 ±10	1710 ±60	-75.6 ±1.3	0.06747 ±0.00071	8265 ±91	8229 ±94	-77.3 ±1.4	**8174 ±94**
DA5-7	876.5	490.1 ±0.6	329 ±6	1670 ±30	-74.0 ±1.2	0.06797 ±0.00039	8314 ±50	8277 ±56	-75.8 ±1.2	**8222 ±56**
DA5-8	876.5	610.6 ±0.7	394 ±6	1730 ±30	-78.0 ±1.1	0.06756 ±0.00041	8300 ±53	8264 ±58	-79.9 ±1.2	**8209 ±58**
DA-15 [n]	879.5	690.7 ±0.1	538 ±5	1440 ±10	-73.6 ±1.3	0.06816 ±0.00015	8334 ±22	8291 ±31	-75.3 ±1.3	**8236 ±31**
DA5-3	880.5	601.8 ±0.8	290 ±10	2400 ±100	-78.2 ±1.2	0.06771 ±0.00048	8320 ±63	8294 ±65	-80.1 ±1.2	**8239 ±65**
DA5-2	881.5	495.7 ±0.7	460 ±10	1220 ±30	-72.1 ±1.2	0.06847 ±0.00049	8360 ±63	8309 ±71	-73.9 ±1.2	**8254 ±71**
DA5-1	882.5	563.9 ±0.8	470 ±10	1350 ±40	-79.7 ±1.3	0.06795 ±0.00052	8365 ±68	8319 ±74	-81.6 ±1.3	**8264 ±74**
DA5-11	882.5	546.3 ±0.6	623 ±5	1000 ±10	-74.0 ±1.3	0.06881 ±0.00037	8420 ±48	8357 ±63	-75.7 ±1.4	**8302 ±63**
Q5, Qunf Cave, Oman										
Q5-15 [n]	2.0	659.6 ±0.8	250 ±10	2800 ±100	-83.1 ±1.6	0.06592 ±0.00027	8138 ±37	8125 ±38	-85.1 ±1.6	**8069 ±38**
Q5-14 [n]	7.0	646.0 ±0.7	290 ±10	2500 ±100	-75.9 ±1.4	0.06692 ±0.00026	8197 ±36	8183 ±36	-77.7 ±1.4	**8127 ±36**
Q5-19 [n]	11.5	739.4 ±0.7	870 ±10	950 ±10	-71.0 ±1.4	0.06763 ±0.00013	8242 ±21	8205 ±28	-72.7 ±1.4	**8149 ±28**
Q5-6 [n]	17.0	492.1 ±0.1	295 ±4	1840 ±20	-79.3 ±0.4	0.06695 ±0.00015	8234 ±19	8215 ±21	-81.2 ±0.4	**8159 ±21**
Q5-10 [n]	26.0	593.0 ±0.9	970 ±10	681 ±9	-84.9 ±1.8	0.06758 ±0.00022	8368 ±33	8316 ±42	-86.9 ±1.8	**8260 ±42**
Q5-7 [n]	27.0	632.8 ±0.1	530 ±6	1340 ±20	-83.3 ±0.6	0.06791 ±0.00015	8395 ±20	8369 ±24	-85.3 ±0.6	**8313 ±24**
Q5-20 [n]	28.0	661.1 ±0.7	200 ±10	3800 ±200	-83.1 ±1.4	0.06804 ±0.00015	8410 ±24	8400 ±24	-85.1 ±1.4	**8344 ±24**
Q5-21 [n]	36.5	698.1 ±0.6	3350 ±40	242 ±3	-71.2 ±1.5	0.07037 ±0.00018	8592 ±27	8441 ±80	-72.9 ±1.5	**8385 ±80**
Q5-8 [n]	40.5	703.0 ±0.1	1350 ±10	598 ±6	-80.4 ±0.4	0.06949 ±0.00014	8570 ±18	8509 ±35	-82.3 ±0.4	**8453 ±35**

Table DR1 (cont.)

Sample Number	Depth to top (mm)	^{238}U ppb	^{232}Th ppt	^{230}Th / ^{232}Th atomic x10^{-6}	$\delta^{234}U$ measured	^{230}Th / ^{238}U activity	Age (yr) uncorrected	Age (yr) corrected	$\delta^{234}U_{Initial}$ (corrected)	Age (yr, BP) corrected
PX5, Paixão Cave, Brazil										
PX-6 [n]	91.0	1884 ±2	217 ±5	24500 ±600	1363 ±2	0.17128 ±0.00028	8150 ±17	8149 ±17	1394.4 ±2.5	**8091 ±17**
PX-7 [n]	94.0	1382 ±1	136 ±3	28900 ±700	1381 ±2	0.17287 ±0.00028	8162 ±16	8161 ±16	1413.3 ±2.3	**8103 ±16**
PX-8 [n]	97.0	1610 ±2	232 ±5	19900 ±400	1392 ±2	0.17435 ±0.00029	8194 ±17	8192 ±17	1425.0 ±2.5	**8134 ±17**
PX-9 [n]	100.5	2094 ±3	82 ±2	74600 ±2200	1405 ±3	0.17617 ±0.00032	8238 ±18	8237 ±18	1437.9 ±2.7	**8179 ±18**
PX-11 [n]	104.0	2456 ±3	110 ±3	65200 ±1700	1408 ±3	0.17715 ±0.00033	8275 ±19	8274 ±19	1441.2 ±2.6	**8216 ±19**
H14, Hoti Cave, Oman										
H14-10 [n]	160.9	1696.1 ±0.5	584 ±8	5300 ±100	599.9 ±0.4	0.11026 ±0.00034	7764 ±25	7758 ±25	613.2 ±0.4	**7702 ±25**
H14-9 [n]	166.3	1786.9 ±0.5	796 ±8	4100 ±40	596.4 ±0.6	0.11066 ±0.00032	7812 ±23	7804 ±24	609.7 ±0.6	**7748 ±24**
H14-8 [n]	201.2	1700.4 ±0.5	285 ±8	11100 ±300	605.9 ±0.6	0.11253 ±0.00036	7899 ±26	7896 ±26	619.6 ±0.6	**7840 ±26**
H14-7 [n]	215.9	1896.2 ±0.5	118 ±9	30000 ±2200	602.2 ±0.4	0.11268 ±0.00034	7929 ±25	7928 ±25	615.9 ±0.4	**7872 ±25**
H14-6 [n]	238.3	1616.0 ±0.4	222 ±7	13800 ±400	606.0 ±0.5	0.11434 ±0.00033	8029 ±24	8027 ±24	619.9 ±0.5	**7971 ±24**
H14-15 [n]	249.2	1739.4 ±0.1	635 ±6	5140 ±50	588.7 ±0.3	0.11380 ±0.00021	8063 ±15	8056 ±16	602.2 ±0.3	**8000 ±15**
H14-18 [n]	272.2	1507.1 ±0.1	114 ±6	25000 ±1300	593.3 ±0.5	0.11491 ±0.00019	8119 ±14	8118 ±14	607.1 ±0.5	**8062 ±14**
H14-5 [n]	275.9	1543.0 ±0.4	665 ±9	4430 ±60	578.4 ±0.5	0.11560 ±0.00036	8269 ±27	8261 ±27	592.0 ±0.5	**8205 ±27**
H14-19 [n]	276.0	1151.5 ±0.1	314 ±6	7000 ±130	577.9 ±0.4	0.11578 ±0.00019	8266 ±14	8261 ±15	591.6 ±0.4	**8205 ±15**
H14-4 [n]	296.0	2117.9 ±0.6	302 ±7	13600 ±300	589.2 ±0.4	0.11716 ±0.00031	8325 ±23	8323 ±23	603.2 ±0.4	**8267 ±23**
H14-13 [n]	300.0	1849.8 ±0.1	1071 ±5	3300 ±20	566.7 ±0.4	0.11607 ±0.00022	8349 ±17	8338 ±17	580.3 ±0.4	**8282 ±17**
H14-12 [n]	324.9	1270.8 ±0.1	1940 ±5	1272 ±4	568.7 ±0.5	0.11791 ±0.00021	8475 ±16	8447 ±21	582.4 ±0.6	**8391 ±21**
H14-3 [n]	338.1	1851.6 ±0.5	944 ±9	3790 ±40	556.1 ±0.8	0.11696 ±0.00030	8495 ±23	8485 ±24	569.6 ±0.8	**8429 ±24**
H14-2 [n]	361.8	1976.7 ±0.6	10680 ±20	366 ±1	561.6 ±0.6	0.11979 ±0.00035	8676 ±26	8576 ±57	575.4 ±0.6	**8520 ±57**
H14-16 [n]	371.9	1764.3 ±0.1	700 ±30	5000 ±200	564.7 ±0.3	0.11929 ±0.00021	8601 ±16	8593 ±16	578.6 ±0.3	**8537 ±16**
H14-1 [n]	384.7	1939.8 ±0.6	1610 ±10	2370 ±20	552.4 ±0.5	0.11884 ±0.00037	8658 ±28	8642 ±29	566.0 ±0.5	**8586 ±29**
PAD07, Padre cave, Brazil										
B2-8	131	652.9 ±0.8	440 ±20	3100 ±100	905.3 ±2.0	0.12761 ±0.00066	7514 ±41	7503 ±41	924.7 ±2.1	**7448 ±41**
B2-16 [n]	166	782.9 ±0.1	113 ±5	14600 ±700	865.9 ±0.8	0.12802 ±0.00023	7704 ±15	7701 ±15	885.0 ±0.8	**7645 ±15**
B2-7	190	1080 ±2	290 ±10	7600 ±300	770.2 ±2.1	0.12296 ±0.00046	7804 ±32	7800 ±32	787.3 ±2.1	**7745 ±32**
B2-15 [n]	211	789.6 ±0.1	104 ±4	15700 ±600	790.6 ±0.9	0.12538 ±0.00022	7869 ±15	7867 ±15	808.3 ±0.9	**7811 ±15**
B2-6-II	237	979 ±1	130 ±10	16500 ±1500	879.1 ±1.5	0.13355 ±0.00056	7988 ±36	7986 ±36	899.2 ±1.6	**7931 ±36**
B2-14 [n]	256	724.5 ±0.1	100 ±5	15300 ±700	837.2 ±1.0	0.13273 ±0.00020	8126 ±14	8124 ±14	856.6 ±1.0	**8068 ±14**
B2-21 [n]	267	979.3 ±0.8	240 ±10	8700 ±400	785.2 ±2.1	0.12960 ±0.00022	8168 ±17	8164 ±17	803.6 ±2.1	**8108 ±17**
B2-5	274	856 ±1	260 ±10	7300 ±400	814.9 ±2.1	0.13255 ±0.00055	8218 ±37	8214 ±37	834.0 ±2.1	**8159 ±37**
B2-13 [n]	279	890.4 ±0.1	220 ±4	7000 ±200	809.9 ±0.5	0.13207 ±0.00018	8211 ±12	8207 ±12	828.9 ±0.5	**8152 ±12**
B2-9	285	1009 ±1	883 ±5	2400 ±20	731.3 ±1.7	0.12704 ±0.00040	8261 ±28	8246 ±29	748.6 ±1.7	**8191 ±29**
B2-12 [n]	291	918.1 ±0.1	493 ±3	3960 ±20	759.0 ±0.4	0.12917 ±0.00021	8266 ±14	8258 ±14	776.9 ±0.4	**8203 ±15**
B2-4	311	505.9 ±0.7	130 ±20	9400 ±1100	916.2 ±2.7	0.14238 ±0.00073	8363 ±46	8359 ±46	938.1 ±2.8	**8304 ±46**
B2-11 [n]	318	667.2 ±0.1	160 ±3	9500 ±200	859.5 ±0.5	0.13837 ±0.00021	8377 ±13	8374 ±13	880.1 ±0.6	**8319 ±13**
B2-3	337	850 ±1	230 ±20	8300 ±600	800.6 ±2.0	0.13411 ±0.00056	8387 ±38	8382 ±38	819.8 ±2.0	**8327 ±38**
B2-10 [n]	353	776.9 ±0.2	1390 ±4	1323 ±6	900.4 ±0.6	0.14331 ±0.00043	8492 ±26	8465 ±30	922.2 ±0.6	**8410 ±30**
B2-2	362	946 ±1	3390 ±20	663 ±4	902.7 ±2.0	0.14405 ±0.00057	8527 ±36	8473 ±45	924.5 ±2.0	**8418 ±45**
B2-1	398	908 ±1	2440 ±10	886 ±6	892.9 ±2.2	0.14457 ±0.00057	8605 ±36	8564 ±42	914.8 ±2.2	**8509 ±42**

Corrected ^{230}Th ages of stalagmites Q5, H14 and PAD0 assume the initial $^{230}Th/^{232}Th$ atomic ratio of 4.4 ±2.2 x10^{-6}. Those are the values for a material at secular equilibrium with the bulk earth $^{232}Th/^{238}U$ value of 3.8. The errors are arbitrarily assumed to be 50%. Corrected ^{230}Th ages of stalagmite D4 and DA assume the initial $^{230}Th/^{232}Th$ atomic ratio of 7 ±5 x10-6 according to ref. S2. *B.P. stands for "Before Present" where the "Present" is defined as the year 1950 A.D.

[n] Measured on a multi-collector inductively coupled plasma mass spectrometers (MC-ICPMS) (Thermo-Finnigan Neptune) and the rest on an ICPMS (Thermo-Finnigan Element).

Table DR2. Oxygen isotopic data of stalagmites D and DA from Dongge Cave, China, Q5 from Qunf Cave, Oman; H14 Hoti Cave, Oman, PAD07 from Padre Cave, Brazil and PX5 from Paixão Cave, Brazil. Depths measured along the growth axis are relative to the top (youngest surface) of stalagmites D4, DA, H14 and PAD07, and relative to first $\delta^{18}O$ point of stalagmite Q5. Ages are established using ^{230}Th ages (see Table S1, and method descriptions). "BP" stands for "Before Present" where the "Present" is defined as the year 1950 A.D.

Depth (mm)	Age (yr, BP)	$\delta^{18}O$ (VPDB)	Depth (mm)	Age (yr, BP)	$\delta^{18}O$ (VPDB)	Depth (mm)	Age (yr, BP)	$\delta^{18}O$ (VPDB)
D4, Dongge Cave, China								
1395.0	7992	-8.96	1433.0	8199	-8.51	1457.5	8278	-9.41
1396.0	7999	-9.20	1434.0	8202	-8.80	1458.0	8280	-9.24
1397.0	8007	-8.91	1434.5	8204	-8.96	1458.5	8281	-8.94
1398.0	8014	-8.84	1435.0	8206	-8.84	1459.0	8282	-8.93
1400.0	8027	-8.91	1435.5	8208	-8.71	1459.5	8284	-8.90
1401.0	8034	-9.26	1436.0	8210	-8.68	1460.0	8285	-8.89
1402.0	8040	-9.01	1436.5	8212	-8.65	1460.5	8286	-8.93
1403.0	8047	-8.75	1437.0	8214	-8.68	1461.0	8288	-8.83
1405.0	8059	-8.82	1437.5	8216	-8.76	1461.5	8289	-8.96
1406.0	8066	-9.13	1438.0	8217	-8.64	1462.0	8290	-8.98
1407.0	8072	-8.70	1438.5	8219	-8.76	1462.5	8292	-9.02
1408.0	8078	-8.59	1439.0	8221	-8.65	1463.0	8293	-8.77
1409.0	8083	-8.95	1439.5	8223	-9.02	1463.5	8294	-8.95
1410.0	8089	-8.14	1440.0	8224	-8.96	1464.0	8296	-9.35
1411.0	8095	-8.63	1440.5	8226	-8.96	1464.5	8297	-9.42
1412.0	8100	-8.69	1441.0	8228	-8.87	1465.0	8298	-9.40
1413.0	8106	-8.80	1441.5	8230	-8.86	1465.5	8299	-9.19
1414.5	8114	-8.70	1442.0	8231	-8.70	1466.0	8301	-9.03
1415.5	8119	-8.61	1442.5	8233	-9.13	1466.5	8302	-9.31
1416.0	8122	-8.70	1443.0	8235	-8.98	1467.0	8303	-9.01
1417.0	8127	-8.80	1443.5	8236	-9.02	1467.5	8304	-9.14
1418.0	8132	-8.74	1444.0	8238	-8.93	1468.0	8306	-8.81
1419.0	8137	-8.71	1444.5	8240	-8.76	1468.5	8307	-9.33
1419.5	8139	-8.70	1445.0	8241	-8.65	1469.0	8308	-9.18
1420.0	8142	-8.93	1445.5	8243	-8.97	1469.5	8309	-8.80
1420.5	8144	-8.64	1446.0	8244	-8.85	1470.0	8310	-9.33
1421.0	8147	-8.47	1446.5	8246	-9.08	1470.5	8312	-8.69
1421.5	8149	-8.64	1447.0	8248	-8.94	1471.0	8313	-8.55
1422.0	8151	-8.86	1447.5	8249	-8.80	1471.5	8314	-8.70
1422.5	8154	-8.18	1448.0	8251	-8.91	1472.0	8315	-8.95
1423.0	8156	-8.26	1448.5	8252	-8.97	1472.5	8317	-8.83
1424.0	8161	-8.71	1449.0	8254	-9.16	1473.0	8318	-8.98
1424.5	8163	-8.71	1449.5	8255	-9.13	1473.5	8319	-9.40
1425.0	8165	-8.67	1450.0	8257	-9.20	1474.0	8320	-8.94
1425.5	8167	-8.58	1450.5	8258	-9.04	1474.5	8321	-8.80
1426.0	8170	-8.72	1451.0	8260	-8.96	1475.0	8322	-8.85
1426.5	8172	-8.61	1451.5	8261	-9.26	1475.5	8324	-9.02
1427.0	8174	-8.70	1452.0	8263	-9.04	1476.0	8325	-8.92
1427.5	8176	-8.83	1452.5	8264	-8.98	1476.5	8326	-9.29
1428.0	8178	-8.44	1453.0	8266	-8.87	1477.0	8327	-8.96
1429.0	8182	-8.45	1453.5	8267	-9.11	1477.5	8328	-8.97
1429.5	8184	-8.57	1454.0	8269	-9.39	1478.0	8330	-8.85
1430.0	8187	-8.68	1454.5	8270	-9.27	1478.5	8331	-8.91
1430.5	8189	-8.56	1455.0	8271	-9.32	1479.0	8332	-8.84
1431.0	8191	-8.57	1455.5	8273	-9.06	1480.0	8334	-9.13
1431.5	8193	-8.56	1456.0	8274	-9.26	1480.5	8335	-9.33
1432.0	8195	-8.69	1456.5	8276	-9.21	1481.0	8337	-9.39
1432.5	8197	-8.49	1457.0	8277	-9.36	1481.5	8338	-9.45

Table DR2 (Cont.)

Depth (mm)	Age (yr, BP)	$\delta^{18}O$ (VPDB)	Depth (mm)	Age (yr, BP)	$\delta^{18}O$ (VPDB)	Depth (mm)	Age (yr, BP)	$\delta^{18}O$ (VPDB)
D4, Dongge Cave, China (cont.)								
1482.0	8339	-9.14	1490.5	8359	-8.80	1499.0	8379	-8.71
1482.5	8340	-9.02	1491.0	8360	-8.63	1499.5	8381	-8.78
1483.0	8341	-9.15	1491.5	8361	-8.80	1500.0	8382	-8.56
1483.5	8342	-8.87	1492.0	8362	-8.84	1500.5	8383	-8.75
1484.0	8344	-8.76	1492.5	8363	-8.73	1501.0	8384	-8.71
1484.5	8345	-8.88	1493.0	8365	-8.95	1501.5	8386	-8.92
1485.0	8346	-8.73	1493.5	8366	-8.80	1502.0	8387	-9.01
1485.5	8347	-8.97	1494.0	8367	-9.03	1502.5	8388	-8.80
1486.0	8348	-8.88	1494.5	8368	-8.85	1503.0	8390	-9.24
1486.5	8349	-8.64	1495.0	8370	-8.91	1508.0	8403	-8.94
1487.0	8351	-8.91	1495.5	8371	-8.90	1513.0	8417	-9.07
1487.5	8352	-9.05	1496.0	8372	-8.82	1518.0	8432	-8.96
1488.0	8353	-8.84	1496.5	8373	-8.30	1523.0	8448	-9.07
1488.5	8354	-9.07	1497.0	8374	-8.31	1528.0	8466	-9.41
1489.0	8355	-9.20	1497.5	8376	-8.99	1533.0	8485	-9.20
1489.5	8356	-9.05	1498.0	8377	-8.91			
1490.0	8358	-8.87	1498.5	8378	-8.74			
DA, Dongge Cave, China								
858.5	7990	-8.79	866.8	8118	-8.49	875.2	8201	-8.27
858.8	7996	-8.64	867.0	8121	-8.37	875.5	8204	-8.14
859.0	8000	-8.72	867.3	8124	-8.57	875.7	8206	-8.28
859.3	8006	-8.65	867.5	8126	-8.49	876.0	8208	-8.48
859.5	8009	-8.81	867.8	8130	-8.41	876.2	8210	-8.16
859.8	8015	-8.78	868.0	8132	-8.34	876.5	8213	-8.24
860.0	8019	-8.78	868.3	8135	-8.51	876.7	8215	-8.24
860.3	8024	-8.71	868.5	8137	-8.35	877.0	8217	-8.20
860.5	8028	-8.84	868.8	8141	-8.47	877.2	8219	-8.39
860.8	8033	-8.73	869.0	8143	-8.48	877.5	8222	-8.26
861.0	8037	-8.70	869.3	8146	-8.55	877.7	8224	-8.19
861.3	8042	-8.64	869.5	8148	-8.50	878.0	8227	-8.45
861.5	8045	-8.81	869.8	8151	-8.57	878.2	8229	-8.35
861.8	8050	-8.65	870.0	8153	-8.37	878.5	8232	-8.35
862.0	8053	-8.78	870.3	8156	-8.78	878.7	8234	-8.27
862.3	8058	-8.62	870.5	8158	-8.33	879.0	8237	-8.30
862.5	8061	-8.62	870.8	8161	-8.66	879.2	8239	-8.48
862.8	8065	-8.57	871.0	8163	-8.42	879.5	8242	-8.41
863.0	8068	-8.37	871.3	8165	-8.66	879.7	8244	-8.43
863.3	8073	-7.94	871.5	8167	-8.56	880.0	8247	-8.48
863.5	8076	-7.96	871.8	8170	-8.69	880.2	8249	-8.61
863.8	8080	-7.97	872.0	8172	-8.34	880.5	8252	-8.45
864.0	8083	-8.10	872.3	8175	-8.48	880.7	8254	-8.53
864.3	8087	-8.21	872.5	8177	-8.26	881.0	8257	-8.46
864.5	8090	-8.28	872.8	8179	-8.64	881.2	8259	-8.48
864.8	8094	-8.27	873.0	8181	-8.48	881.5	8263	-8.51
865.0	8096	-8.40	873.5	8186	-8.49	881.7	8265	-8.52
865.3	8100	-8.53	873.7	8187	-8.19	882.0	8268	-8.64
865.5	8103	-8.41	874.0	8190	-8.38	882.5	8274	-8.67
865.8	8106	-8.39	874.2	8192	-8.22	882.5	8280	-8.63
866.0	8109	-8.25	874.5	8195	-8.27	882.5	8286	-8.75
866.3	8113	-8.43	874.7	8196	-8.27	882.5	8293	-8.78
866.5	8115	-8.50	875.0	8199	-8.13	882.5	8299	-8.77

Table DR2 (Cont.)

Depth (mm)	Age (yr, BP)	$\delta^{18}O$ (VPDB)	Depth (mm)	Age (yr, BP)	$\delta^{18}O$ (VPDB)	Depth (mm)	Age (yr, BP)	$\delta^{18}O$ (VPDB)
DA, Dongge Cave, China (cont.)								
882.5	8306	-8.78	882.5	8321	-8.88	884.5	8336	-8.88
882.5	8313	-8.80	883.5	8328	-8.99	885.5	8344	-8.98
Q5, Qunf Cave, Oman								
0.0	8030	-1.89	14.5	8154	-1.59	29.5	8354	-2.40
1.0	8050	-1.85	17.0	8159	-1.58	31.0	8365	-2.33
3.0	8088	-1.55	19.5	8193	-1.48	32.5	8375	-2.22
4.5	8108	-1.80	21.5	8226	-1.64	36.5	8385	-2.32
7.0	8127	-1.86	26.0	8260	-1.92	40.5	8453	-1.75
9.5	8138	-1.68	27.0	8313	-2.04			
11.5	8149	-1.66	28.0	8344	-2.29			
H14, Hoti Cave, Oman								
153.8	7678	-4.08	173.4	7768	-4.54	194.1	7834	-4.82
154.3	7680	-4.08	174.0	7771	-4.37	194.7	7835	-4.86
154.8	7682	-4.23	174.5	7774	-4.67	195.2	7837	-4.92
155.3	7684	-4.10	175.1	7777	-4.38	195.8	7839	-4.98
155.8	7687	-4.15	175.6	7779	-4.55	196.3	7840	-5.07
156.3	7689	-3.78	176.2	7780	-4.31	196.9	7842	-5.17
156.8	7691	-4.00	176.7	7782	-4.30	197.4	7844	-5.18
157.4	7693	-4.33	177.3	7784	-4.14	198.0	7846	-5.02
157.4	7695	-4.61	177.8	7786	-4.27	198.5	7847	-5.04
157.9	7697	-4.35	178.3	7787	-4.22	199.0	7849	-5.09
158.4	7698	-4.16	178.9	7789	-4.33	199.6	7851	-5.11
158.9	7700	-4.47	179.4	7791	-4.10	200.1	7853	-5.07
159.4	7702	-4.33	180.0	7792	-4.51	200.7	7854	-5.13
159.9	7704	-4.15	180.5	7794	-4.65	201.2	7856	-5.09
160.4	7705	-4.70	181.1	7796	-4.42	201.8	7857	-4.91
160.9	7707	-4.56	181.6	7797	-4.29	202.3	7859	-4.88
161.5	7710	-4.26	182.2	7799	-4.52	202.9	7860	-4.88
162.0	7713	-4.20	182.7	7801	-4.57	203.4	7862	-4.82
162.5	7716	-4.22	183.2	7802	-4.42	203.9	7863	-4.85
163.1	7719	-4.22	183.8	7804	-4.77	204.5	7865	-4.95
163.6	7721	-3.93	184.3	7806	-4.79	205.0	7866	-5.05
164.2	7724	-4.36	184.9	7807	-4.70	205.6	7868	-5.00
164.7	7727	-4.54	185.4	7809	-4.53	206.1	7869	-4.95
165.3	7730	-4.09	186.0	7810	-4.75	206.7	7871	-5.08
165.8	7732	-4.66	186.5	7812	-4.65	207.2	7872	-4.96
166.4	7734	-3.84	187.1	7813	-4.70	207.8	7874	-4.69
166.9	7736	-4.20	187.6	7815	-4.37	208.3	7875	-4.39
167.5	7738	-4.21	188.2	7816	-4.75	208.8	7877	-4.36
168.0	7741	-4.31	188.7	7818	-4.88	209.4	7878	-3.99
168.5	7743	-4.62	189.2	7819	-4.64	209.9	7880	-4.14
169.1	7745	-5.25	189.8	7821	-4.69	210.5	7881	-4.28
169.6	7747	-4.62	190.3	7822	-4.68	211.0	7883	-4.37
170.2	7749	-4.41	190.9	7824	-4.78	211.6	7885	-4.35
170.7	7752	-3.97	191.4	7825	-4.87	212.1	7887	-4.28
171.3	7755	-3.85	192.0	7827	-4.92	212.7	7889	-4.29
171.8	7758	-4.57	192.5	7829	-4.92	213.2	7891	-4.26
172.4	7761	-4.57	193.1	7830	-5.01	213.8	7892	-4.18
172.9	7765	-4.39	193.6	7832	-4.85	214.3	7894	-4.13

Table DR2 (Cont.)

Depth (mm)	Age (yr, BP)	$\delta^{18}O$ (VPDB)	Depth (mm)	Age (yr, BP)	$\delta^{18}O$ (VPDB)	Depth (mm)	Age (yr, BP)	$\delta^{18}O$ (VPDB)
H14, Hoti Cave, Oman (cont.)								
214.8	7896	-4.25	242.6	7971	-5.47	270.4	8058	-4.27
215.4	7898	-4.31	243.2	7973	-5.31	270.9	8060	-4.26
215.9	7900	-4.40	243.7	7974	-5.11	271.5	8062	-4.38
216.5	7902	-4.39	244.3	7975	-5.11	272.0	8064	-4.20
217.0	7904	-4.44	244.8	7977	-5.03	272.6	8065	-4.33
217.6	7905	-4.38	245.3	7978	-5.15	273.1	8067	-4.03
218.1	7907	-4.40	245.9	7980	-5.13	273.7	8069	-3.70
218.7	7909	-4.33	246.4	7981	-5.23	274.2		
219.2	7911	-4.34	247.0	7983	-5.27	274.8	8193	-3.06
219.7	7912	-4.26	247.5	7985	-5.03	275.3	8196	-3.36
220.3	7914	-4.18	248.1	7986	-5.15	275.9	8199	-3.78
220.8	7916	-4.38	248.6	7988	-5.19	276.4	8203	-4.23
221.4	7917	-4.51	249.2	7990	-5.20	276.9	8206	-3.94
221.9	7919	-4.34	249.7	7991	-4.84	277.5	8209	-3.66
222.5	7920	-4.66	250.2	7993	-4.77	278.0	8212	-3.94
223.0	7922	-4.75	250.8	7995	-4.84	278.6	8215	-4.07
223.6	7923	-4.83	251.3	7996	-4.96	279.1	8219	-4.12
224.1	7925	-4.83	251.9	7998	-4.82	279.7	8222	-4.11
224.6	7926	-4.54	252.4	8000	-4.86	280.2	8225	-4.11
225.2	7928	-4.66	253.0	8001	-4.86	280.8	8227	-4.13
225.7	7929	-4.69	253.5	8003	-4.98	281.3	8229	-3.82
226.3	7931	-4.75	254.1	8005	-5.00	281.8	8230	-3.85
226.8	7932	-4.80	254.6	8006	-5.09	282.4	8232	-3.85
227.4	7934	-4.96	255.2	8008	-5.12	282.9	8234	-3.87
227.9	7935	-5.03	255.7	8010	-5.20	283.5	8236	-3.83
228.5	7937	-5.03	256.2	8012	-5.08	284.0	8237	-4.02
229.0	7938	-5.04	256.8	8013	-4.97	284.6	8239	-4.05
229.5	7940	-5.08	257.3	8015	-4.55	285.1	8241	-4.07
230.1	7941	-5.06	257.9	8017	-4.97	285.7	8243	-4.26
230.6	7942	-5.08	258.4	8019	-4.90	286.2	8244	-4.28
231.2	7944	-5.19	259.0	8021	-4.63	286.7	8246	-4.26
231.7	7945	-5.17	259.5	8022	-5.07	287.3	8247	-4.33
232.3	7946	-5.22	260.1	8024	-5.11	287.8	8249	-4.33
232.8	7948	-5.21	260.6	8026	-5.20	288.4	8250	-4.27
233.4	7949	-5.30	261.1	8028	-5.11	288.9	8252	-4.42
233.9	7950	-5.32	261.7	8030	-5.07	289.5	8253	-4.40
234.5	7952	-5.28	262.2	8031	-4.97	290.0	8255	-4.50
235.0	7953	-5.23	262.8	8033	-5.07	290.6	8257	-4.38
235.5	7954	-5.34	263.3	8035	-5.05	291.1	8259	-4.41
236.1	7956	-5.27	263.9	8037	-5.01	291.6	8260	-4.36
236.6	7957	-5.19	264.4	8038	-4.72	292.2	8262	-4.44
237.2	7958	-5.32	265.0	8040	-4.85	292.7	8264	-4.41
237.7	7960	-5.19	265.5	8042	-4.88	293.3	8266	-4.55
238.3	7961	-5.36	266.0	8044	-4.69	293.8	8268	-4.59
238.8	7962	-5.30	266.6	8045	-4.56	294.4	8269	-4.59
239.4	7963	-4.97	267.1	8047	-4.35	294.9	8271	-4.62
239.9	7965	-5.16	267.7	8049	-4.54	295.5	8273	-4.76
240.4	7966	-5.26	268.2	8051	-4.47	296.0	8274	-4.78
241.0	7967	-5.28	268.8	8053	-4.55	296.6	8276	-4.98
241.5	7969	-5.37	269.3	8055	-4.30	297.1	8277	-5.31
242.1	7970	-5.42	269.9	8056	-4.14	297.6	8279	-5.40

Table DR2 (Cont.)

Depth (mm)	Age (yr, BP)	$\delta^{18}O$ (VPDB)	Depth (mm)	Age (yr, BP)	$\delta^{18}O$ (VPDB)	Depth (mm)	Age (yr, BP)	$\delta^{18}O$ (VPDB)
H14, Hoti Cave, Oman (cont.)								
298.2	8280	-4.96	320.5	8353	-3.76	351.6	8465	-4.47
298.7	8282	-5.04	321.1	8354	-3.46	352.5	8468	-4.54
299.3	8283	-4.70	321.6	8358	-3.82	353.3	8470	-4.66
299.8	8285	-4.66	322.2	8362	-4.19	354.2	8472	-4.67
300.4	8286	-4.89	322.7	8366	-4.28	355.0	8474	-4.48
300.9	8288	-4.98	323.2	8370	-4.22	355.9	8477	-4.52
301.5	8289	-4.95	323.8	8374	-4.16	356.7	8479	-4.52
302.0	8291	-4.94	324.3	8378	-3.88	357.5	8482	-4.93
302.5	8292	-4.76	324.9	8381	-3.76	358.4	8484	-4.96
303.1	8294	-4.79	325.4	8385	-3.36	359.2	8487	-5.12
303.6	8296	-4.79	326.0	8389	-2.89	360.1	8489	-4.99
304.2	8297	-3.91	326.5	8393	-2.61	360.9	8491	-5.20
304.7	8299	-4.69	327.1	8395	-2.73	361.8	8493	-5.14
305.3	8300	-4.74	327.9	8397	-4.47	362.6	8495	-4.90
305.8	8302	-4.88	328.8	8399	-4.40	363.5	8498	-4.76
306.4	8304	-4.90	329.6	8401	-4.45	364.3	8500	-4.24
306.9	8306	-4.87	330.4	8403	-4.69	365.2	8502	-4.12
307.4	8308	-4.75	331.3	8405	-4.82	366.0	8504	-4.15
308.0	8310	-4.79	332.1	8407	-4.73	366.9	8507	-4.42
308.5	8312	-3.96	333.0	8409	-5.19	367.7	8510	-4.34
309.1	8314	-4.22	333.8	8411	-4.94	368.6	8513	-4.37
309.6	8316	-4.35	334.7	8413	-4.81	369.4	8516	-4.36
310.2	8318	-4.51	335.5	8415	-5.34	370.3	8519	-4.53
310.7	8320	-4.58	336.4	8418	-4.94	371.1	8522	-4.45
311.3	8322	-4.58	337.2	8422	-4.30	371.9	8525	-4.49
311.8	8324	-4.40	338.1	8425	-4.69	372.8	8527	-4.54
312.3	8326	-4.57	338.9	8429	-4.76	373.6	8530	-4.78
312.9	8328	-4.59	339.8	8432	-4.78	374.5	8532	-4.71
313.4	8330	-4.74	340.6	8434	-4.85	375.3	8534	-4.70
314.0	8332	-4.69	341.5	8437	-4.80	376.2	8537	-4.63
314.5	8334	-4.68	342.3	8439	-4.93	377.0	8539	-4.71
315.1	8336	-4.63	343.1	8442	-4.84	377.9	8541	-4.68
315.6	8338	-4.71	344.0	8444	-4.83	378.7	8543	-4.65
316.2	8339	-4.64	344.8	8447	-4.66	379.6	8546	-4.90
316.7	8341	-4.60	345.7	8449	-4.61	380.4	8548	-5.16
317.3	8343	-4.58	346.5	8451	-4.58	381.3	8552	-5.04
317.8	8344	-4.30	347.4	8454	-4.65	382.1	8555	-4.91
318.3	8346	-4.19	348.2	8456	-4.71	383.0	8559	-4.88
318.9	8348	-4.20	349.1	8459	-4.54	383.8	8562	-4.77
319.4	8349	-4.31	349.9	8461	-4.59	384.7	8566	-4.59
320.0	8351	-4.13	350.8	8463	-4.52			
PAD07, Padre Cave, Brazil								
199.0	7782	-6.151	209.5	7833	-5.62	220.3	7886	-6.04
200.5	7789	-6.372	210.5	7838	-6.02	221.5	7892	-6.46
202.0	7797	-6.474	211.8	7844	-6.57	222.5	7896	-6.11
203.5	7804	-6.387	213.0	7850	-7.02	223.5	7901	-6.47
205.0	7811	-5.710	214.5	7858	-6.35	224.5	7906	-6.24
206.5	7819	-5.995	216.0	7865	-6.27	225.5	7911	-6.24
207.5	7823	-6.000	217.5	7872	-6.23	226.8	7917	-6.43
208.5	7828	-5.768	219.0	7879	-6.12	228.0	7923	-6.42

Table DR2 (Cont.)

Depth (mm)	Age (yr, BP)	$\delta^{18}O$ (VPDB)	Depth (mm)	Age (yr, BP)	$\delta^{18}O$ (VPDB)	Depth (mm)	Age (yr, BP)	$\delta^{18}O$ (VPDB)
PAD07, Padre Cave, Brazil (cont.)								
229.3	7929	-6.29	286.3	8186	-7.71	331.3	8351	-6.11
230.5	7935	-5.79	287.0	8189	-8.11	332.0	8353	-6.26
231.5	7940	-6.20	288.3	8194	-8.13	333.3	8358	-6.27
232.5	7944	-5.80	289.5	8199	-7.49	334.7	8362	-6.27
233.8	7950	-6.26	290.2	8202	-7.32	336.0	8366	-6.08
235.0	7956	-6.32	290.8	8205	-7.46	336.3	8366	-6.05
237.2	7967	-5.82	291.5	8207	-7.53	337.3	8369	-6.15
237.8	7970	-6.03	292.0	8209	-7.68	338.0	8372	-6.65
238.5	7973	-6.86	292.5	8211	-7.67	339.2	8375	-6.48
239.5	7978	-6.87	293.0	8213	-6.67	340.3	8379	-6.43
240.5	7982	-7.08	294.3	8218	-6.83	341.5	8382	-5.96
242.3	7991	-5.81	295.5	8223	-6.69	342.3	8384	-5.96
244.0	7999	-7.29	296.2	8226	-6.71	343.2	8387	-6.14
245.3	8005	-6.05	296.8	8228	-6.80	344.0	8389	-6.41
246.5	8010	-6.89	297.5	8231	-6.49	345.2	8392	-6.34
247.7	8016	-6.42	298.5	8235	-6.63	346.3	8396	-6.42
248.8	8021	-6.72	299.5	8239	-6.30	347.5	8399	-6.01
250.0	8027	-6.46	301.3	8246	-6.34	348.3	8401	-5.86
251.8	8035	-6.73	303.0	8252	-6.93	349.2	8403	-6.06
253.5	8043	-6.60	303.5	8254	-6.72	350.0	8405	-6.39
254.5	8047	-6.59	304.0	8256	-7.71	350.9	8408	-6.80
255.5	8052	-6.79	304.5	8258	-6.11	351.8	8410	-6.60
256.5	8056	-7.32	306.0	8264	-6.63	352.7	8412	-6.43
257.8	8062	-6.94	307.5	8269	-5.79	352.9	8413	-6.09
259.0	8068	-6.60	308.2	8272	-6.38	354.3	8416	-5.80
260.5	8075	-6.66	308.8	8274	-6.34	355.5	8419	-5.39
262.0	8081	-6.91	309.5	8277	-6.78	356.5	8422	-4.94
262.8	8085	-6.83	310.5	8280	-6.08	357.5	8424	-5.71
263.7	8089	-6.75	311.5	8284	-6.53	358.5	8427	-5.59
264.5	8092	-7.00	312.5	8288	-5.95	360.0	8430	-5.74
265.5	8097	-7.40	313.0	8289	-6.44	362.3	8436	-5.73
266.5	8101	-7.86	313.5	8291	-6.31	363.2	8438	-6.60
267.8	8107	-7.89	314.0	8293	-6.48	364.0	8439	-6.82
269.0	8112	-6.89	314.5	8295	-6.65	365.5	8443	-6.66
270.0	8117	-5.97	315.3	8298	-6.94	367.0	8446	-6.93
271.0	8121	-6.52	316.2	8301	-7.29	367.8	8447	-6.40
273.0	8130	-6.33	317.0	8304	-7.24	368.5	8449	-7.07
273.6	8132	-6.22	318.2	8308	-7.41	370.5	8453	-6.94
275.5	8141	-6.51	318.8	8310	-7.45	372.5	8457	-7.55
276.3	8144	-6.39	319.5	8312	-7.59	373.5	8459	-6.82
277.0	8147	-6.96	320.5	8316	-7.15	374.5	8461	-7.37
277.8	8150	-6.65	321.5	8319	-6.88	375.5	8463	-7.25
278.5	8153	-7.39	322.5	8322	-6.22	376.3	8464	-7.28
279.5	8158	-7.27	323.8	8327	-6.12	377.2	8466	-7.43
280.5	8162	-7.71	325.0	8331	-6.20	378.0	8467	-6.20
281.3	8165	-7.50	326.0	8334	-6.38	379.0	8469	-6.25
282.0	8168	-8.20	327.0	8337	-6.18	380.0	8471	-6.71
282.8	8171	-7.87	328.0	8341	-6.43	380.5	8471	-6.48
283.5	8174	-7.76	329.0	8344	-6.39	381.0	8472	-6.48
285.0	8181	-8.12	330.0	8347	-6.21	381.8	8474	-6.35
285.5	8183	-7.84	330.7	8349	-6.19	382.7	8475	-6.71

Table DR2 (Cont.)

Depth (mm)	Age (yr, BP)	$\delta^{18}O$ (VPDB)	Depth (mm)	Age (yr, BP)	$\delta^{18}O$ (VPDB)	Depth (mm)	Age (yr, BP)	$\delta^{18}O$ (VPDB)
PAD07, Padre Cave, Brazil (cont.)								
383.5	8476	-6.99	393.5	8490	-6.81	406.0	8502	-6.49
384.5	8478	-7.00	394.5	8491	-6.24	407.5	8503	-6.19
385.5	8479	-7.19	395.5	8492	-6.11	409.8	8504	-6.21
386.5	8481	-7.22	396.5	8493	-6.67	412.0	8505	-6.43
387.5	8482	-7.10	397.0	8494	-6.51	416.0	8507	-6.45
388.5	8483	-6.70	400.3	8497	-6.14	421.0	8507	-6.49
389.5	8485	-6.60	403.0	8499	-5.77			
390.3	8486	-6.45	404.5	8501	-6.40			
PX5, Paixão Cave, Brazil								
90.0	8087	-5.07	95.0	8114	-5.93	101.0	8185	-5.97
90.5	8089	-5.37	95.5	8119	-6.13	101.5	8190	-5.79
91.0	8091	-5.49	96.0	8124	-6.05	102.0	8195	-5.49
91.5	8093	-5.57	96.5	8129	-4.87	102.5	8200	-5.20
92.0	8095	-4.79	97.0	8134	-5.09	103.0	8206	-5.21
92.5	8097	-4.17	98.0	8147	-5.04	103.5	8211	-4.97
93.0	8099	-4.86	98.5	8154	-5.13	104.0	8216	-3.58
93.5	8101	-4.51	99.5	8166	-6.76	104.5	8221	-4.63
94.0	8103	-4.16	100.0	8173	-7.26			
94.5	8108	-6.84	100.5	8179	-6.23			

4. References Cited

Cheng H. Edwards, R.L., Hoff, J., Gallup, C.D., Richards, D.A. and Asmerom Y., 2000, The half-lives of uranium-234 and thorium-230: Chemical Geology, v. 169, p. 17–33.

Cheng, H. Edwards, R.L., Shen, C.C., Woodhead, J., Hellstrom, J., Wang, Y.J., Kong, X.G., Wang, X.F., 2008, A new generation of Th-230 dating techniques: Tests of precision and accuracy: GEOCHIMICA ET COSMOCHIMICA ACTA v. 72, p. A157–A157.

Cheng, H., Edwards, R.L., Shen, C.C., Woodhead, J., Hellstrom, J., Wang, Y.J., Kong, X.G., and Wang, X.F., A new generation of ^{230}Th dating techniques: a test of dating precision and accuracy: To be submitted to Earth and Plant. Sci. Lett. (2009).

Dykoski, C.A., Edwards, R.L., Cheng, H., Yuan, D.X., Cai, Y.J., Zhang, M.L., Lin, Y.S., An, Z.S., and Revenaugh, J.2005, A high-resolution, absolute-dated Holocene and deglacial Asian monsoon record from Dongge Cave, China: Earth Planet. Sci. Letters, v. 233, p. 71– 86.

Edwards, R.L., Chen, J.H., and Wasserburg, G.J., 1987, ^{238}U–^{234}U–^{230}Th–^{232}Th systematics and the precise measurement of time over the past 500,000 years: Earth Planet. Sci. Lett., v. 81, p. 175–192.

Fleitmann, D., Burns, S.J., Mudelsee, M., Neff, U., Kramers, J., Mangini, A., Matter, A., 2003, Holocene forcing of the Indian Monsoon recorded in a stalagmite from southern Oman: Science, v. 300, p. 1737–1739.

Hughen, K.A., Overpeck, J. T., Peterson, L. C., and Trumbore, S. 1996, Rapid climate changes in the tropical Atlantic region during the last deglaciation: Nature, v. 380, p. 51–54.

Neff, U., Burns, S.J., Mangini, A., Mudelsee, M., Fleitmann, D., and Matter, A., 2001, Strong coherence between solar variability and the monsoon in Oman between 9 and 6 kyr ago: Nature, v. 411, p. 290–293.

Rasmussen, S.O., Andersen, K.K., Svensson, A.M., Steffensen, J.P., Vinther, B.M., Clausen, H.B., Siggaard-Andersen, M.-L., Johnsen, S.J., Larsen, L.B., Dahl-Jensen, D., Bigler, M., Röthlisberger, R., Fischer, H., Goto-Azuma, K., Hansson, M.E., Ruth, U., 2006, A new Greenland ice core chronology for the last glacial termination: Journal of Geophysical Research-Atmospheres, v. 111, D06102, doi: 10.1029/2005JD006079.

Shen, C.-C., Edwards, R.L., Cheng, H., Dorale, J.A., Thomas, R.B., Moran, S.B., Weinstein, S.E., and Edmonds, H.N., 2002. Uranium and thorium isotopic and concentration measurements by magnetic sector inductively coupled plasma mass spectrometry: Chemical Geology, v. 185, p. 165-178.

Spurk, M., Leuschner, H. H., Baillie, M. G. L., Briffa, K.R., and Friedrich, M., 2002, Depositional frequency of German subfossil oaks: climatically and non-climatically induced fluctuations in the Holocene: Holocene, v. 12, p. 707–715.

Stuiver M., Reimer P. J., Bard E., Beck J. W., Burr C. S., Hughen K. A., Kromer B., McCormac G., Plicht J. V. D., and Spurk M.,1998, INTCAL98 Radiocarbon age calibration, 24,000-0 cal BP: Radiocarbon, v. 40, p. 1041–1083.

Stuiver, M. and Grootes, P.M., 2000, GISP2 Oxygen Isotope Ratios: Quaternary Research, v. 53, p. 277–284.

Wang, X.F. Edwards, R.L, Auler, A.S., Cheng, H., and Ito, E., 2007, Millennial-scaleinterhemispheric asymmetry of low-latitude precipitation: speleothem evidence and possible high-latitude forcing. AGU Monograph: Past and Future Changes of the Ocean's Meridional Overturning Circulation: Mechanisms and Impacts. Edited by A. Schmittner, J. Chiang, and S. Hemming. v.173, p. 279–294.

WangY.J., Cheng, H., Edwards, R.L., He, Y.Q., Kong, X.G., An, Z.S., Wu, J.Y., Kelly, M.J., Dykosk, C.A., and Li, X.D., 2005. 2005, The Holocene Asian Monsoon: Links to Solar Changes and North Atlantic Climate: Science, v. 308, p. 854–857.

Wieser, M.E. and Schwieters, J.B., 2005, The development of multiple collector mass spectrometry for isotope ratio measurements: Int. J. Mass Spectrom, v. 242, p. 97–115.

Zhang, R., and Delworth, T.L., 2005, Simulated Tropical Response to a Substantial Weakening of the Atlantic Thermohaline Circulation: Journal of Climate, v. 18, p.1853–1860.